



Karaj branch

## **Preparation and Characterization of Aluminum Nitride Thin Films with the Potential Application in Electro-Acoustic Devices**

**Fatemeh Hajakbari**

*Department of Physics, Karaj Branch, Islamic Azad University, Karaj, Iran*

*(Received 10 Aug. 2019; Final revised received 12 Nov.2019)*

---

### **Abstract**

In this work, aluminum nitride (AlN) thin films with different thicknesses were deposited on quartz and silicon substrates using single ion beam sputtering technique. The physical and chemical properties of prepared films were investigated by different characterization technique. X-ray diffraction (XRD) spectra revealed that all of the deposited films have an amorphous structure. The Al-N bond information of deposited films on silicon substrates was identified by Fourier transform infrared (FTIR) spectroscopy. FTIR results confirmed the formation of AlN films in prepared samples. Atomic force microscopy (AFM) revealed that the surface of films was smooth with low values of roughness. The low values of roughness can be caused the low acoustic loss in AlN films, which is interesting for applications in electro-acoustic devices.

**Keywords:** AlN, Ion beam sputtering, Film thickness, Morphology. Optical properties,

---

## **Introduction**

Aluminum nitride (AlN) thin films due to its many excellent properties such as good thermal and chemical stability, high hardness, high electrical resistivity, high thermal conductivity, wide optical band gap of about 6.2 eV, low toxicity, high ultrasonic velocity and good piezoelectric coefficient [1-6] are being extensively used for diverse applications, such as microelectronic and optoelectronics devices [1-13] especially in surface and bulk acoustic wave devices [8]. A large variety of methods have been used for preparation of AlN thin films on different substrates including DC and RF reactive sputtering [8-10], pulsed laser deposition [11], plasma-enhanced atomic layer deposition [4] and chemical vapor deposition [13]. An alternative method of AlN thin films preparation is single ion beam sputtering method (SIBS) [12].

SIBS method is a kind of physical vapour deposition technique which has many advantages over other sputtering methods, such as independent control over the incident beam energy, the current density and the incidence angle of bombarding ions [12]. The main motivation of this paper is to prepare AlN thin films with different thicknesses on quartz and silicon substrates using single ion beam sputtering technique. The properties of these prepared films show that the films have the potential to be applied in Electro-Acoustic devices and further studies are necessary in order to explain this application of AlN films. On the other hands knowledge of the optical properties of thin films are obviously necessary for application of these films in optoelectronic devices. The optical features of semiconductor films depend on different parameters, such as their preparation conditions and methods [14-24]. The present work focuses on the influence of film thickness on the morphological and optical properties of amorphous AlN thin films. Different characterization methods such as, X-ray diffraction (XRD), atomic force microscopy (AFM), Fourier transform infrared (FTIR) spectroscopy and spectrophotometry have been employed to investigate the effect of films thickness on morphological and optical properties of AlN thin films. The structure of the paper is as follows: after this short introduction, in section 2, the steps taken for production and characterization of AlN thin films by SIBS method are explained. In section 3 and 4, the results and discussions followed by the conclusions are presented.

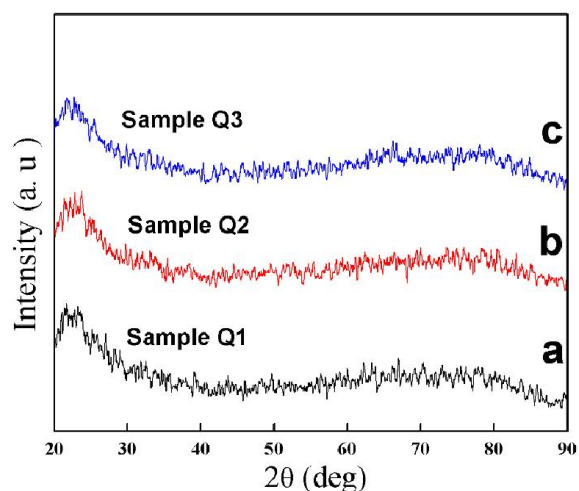
## **Experimental**

The AlN films have been deposited on quartz substrates by means of a single reactive ion beam sputtering system using a pure aluminum target (purity 99.999%) and a mixture of argon (99.999%) and nitrogen (99.999%) gases with equal contents. For preparation of AlN films with different thickness, the deposition times was varied from 10 to 30 minutes while the other deposition parameters were kept constant. Prior to any deposition, the deposition chamber was carefully

cleaned and then evacuated to background pressure of  $6 \times 10^{-6}$  Torr before introducing the gas mixture. The substrate temperature was held at 400 °C during film deposition with using a heater and thermocouple. The substrates were ultrasonically cleaned in acetone and ethanol for about 30 min and dried with dry argon before loading into the deposition chamber. The ion beam energy and ion beam current for sputtering were kept at 2.2 keV and 25mA respectively during the deposition. The working pressure was  $2 \times 10^{-4}$  Torr and the flow rates of argon and nitrogen were kept 25 sccm. The deposition times were 10, 20 and 30 min and the samples were abbreviated as Sample Q1, Sample Q2 and Sample Q3 respectively. The thickness of films measured using a surface profilometer (Detak3) were found to be 50, 80 and 120 nm for samples Q1, Q2 and Q3, respectively. The structural properties of the films were characterized by X-ray diffraction (XRD, PW1800, Philips). The Al-N bond information of deposited film on silicon substrate was identified by Fourier transform infrared (FTIR; Perkin Elmer spectrum 100) spectroscopy. The surface morphology of films was examined by contact mode atomic force microscopy (AFM) (Park Scientific Instrument Auto probe CP). The scan area was  $2 \times 2 \mu\text{m}^2$ . The two dimensional AFM image processing was done using the WSxM program [25]. The optical transmittance and reflectance spectra of the films were measured at normal incidence over the 200-800 nm spectral regions at room temperature, with a spectrophotometer (Varian Inc, CA, USA) to determine the optical characteristics of AlN thin films.

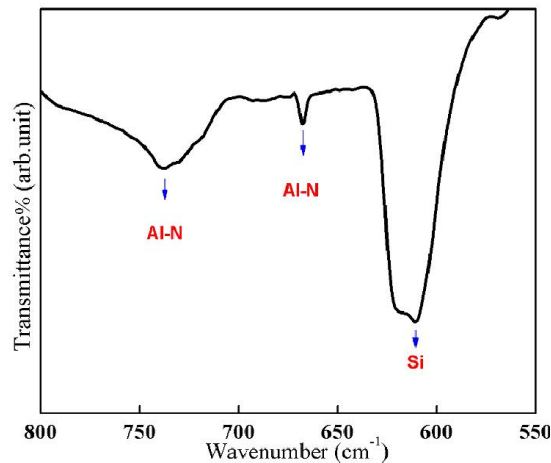
## Results and Discussion

Figure 1 shows the X-ray diffraction patterns of AlN thin films with different thicknesses deposited on quartz substrates. The films show no characteristics XRD peaks except of wide and broad peak at  $22.1^\circ$  related to quartz substrate.



**Figure 1.** X-ray diffraction patterns of AlN films with different thicknesses deposited on quartz substrates: (a) 50 nm, (b) 80 nm and (c) 120 nm.

The absence of distinct diffraction peaks suggest that the films are amorphous in nature. A similar kind of amorphous structure was reported earlier [12]. For Al-N bond information, the FTIR spectrum of AlN thin film deposited on silicon substrate is recorded in a transmittance mode and is shown in Figure 2. From the FTIR spectrum the wavenumber of 668 and 739  $\text{cm}^{-1}$  are associated with the Al-N bonding and a peak appearing at 611  $\text{cm}^{-1}$  is related to the silicon substrate. The FTIR results clearly confirmed that the deposited films were AlN. This result is in good agreement with the result reported by Y. Fu et al [26].



**Figure2.** FTIR transmittance spectrum of AlN film deposited on silicon substrate.

The surface morphology of films was studied by AFM in a contact mode. The AFM results of AlN films with different thicknesses are compared in Figure 3. The AFM pictures show that the surface morphology of the films depends strongly on the AlN film thickness. The smooth and dense surface has been observed for the films deposited in smaller deposition times and by enhancing of the deposition time to 30 min, the pyramidal types of grains were grown perpendicular to the substrate surface. The root mean square roughness ( $R_{\text{rms}}$ ) values, were calculated by a formula [27]:

$$R_{\text{rms}} = \sqrt{\frac{1}{N} \sum (Z_m - Z_i)^2} \quad (1)$$

Where N the number of deviations,  $Z_i$  is the height reference and  $Z_m$  is the profile value. AFM analysis indicates that the root mean square ( $R_{\text{rms}}$ ) surface roughness increased from 1.10 to 1.41 nm when the film thickness varied in the range of 50 to 120 nm.

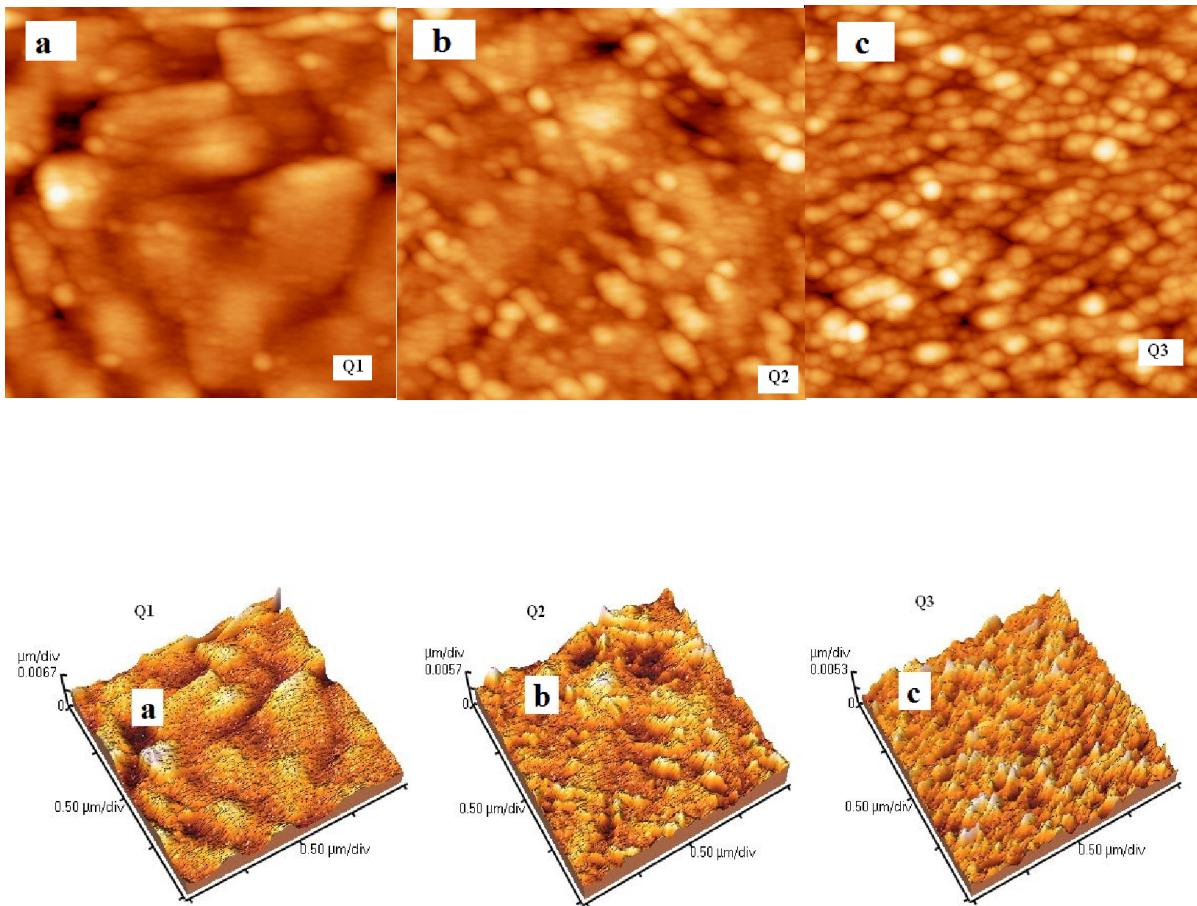


**Figure 3.** 3D and 2D AFM images of AlN films with different thicknesses deposited on quartz substrates: (a) 50 nm, (b) 80 nm and (c) 120 nm.

The low values of roughness can be caused the low acoustic loss in AlN films, which is interesting for applications in electro-acoustic devices, such as surface acoustic wave devices [8, 9]. The acoustic waves present a higher propagation velocity in the case of amorphous structures than in the case of polycrystalline nanostructure ones [9]. Also, the average grain size evaluated from AFM measurements varied in the range of 65 to 100 nm. Also, the roughness values exhibit a similar tendency to that of grain sizes observed from AFM analysis [28, 29]. Therefore, it is apparent, the average surface grain size and  $R_{rms}$  roughness of the films increase with increasing of the film thickness, that exhibited the film thickness, changes the grain size as well as the surface roughness. The topographic height histogram are shown in Fig. 4. The histogram of the surface height distribution profiles shows a shape of Gaussian distribution that confirmed the homogeneity of the films and the surface roughness is increased by peak broadening in the height distribution profiles [20, 23].

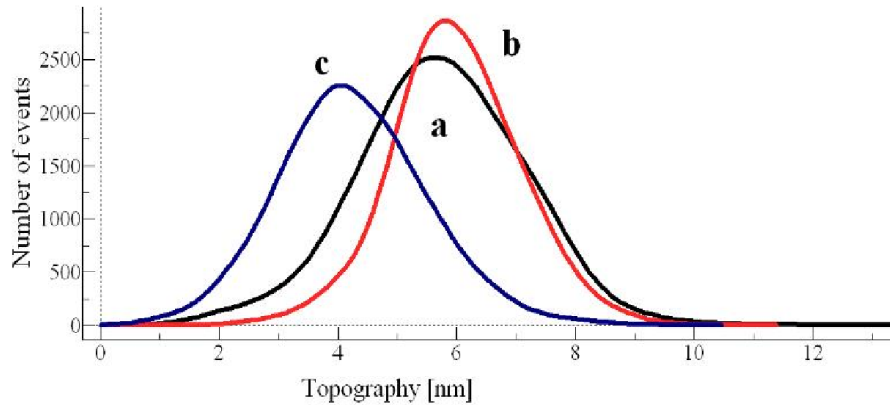


**Figure 4.** Topographic histogram images of AlN thin films with different thicknesses: (a) 50 nm, (b) 80 nm and (c) 120 nm.

Figure 5 presents the optical transmittance (T) and reflectance (R) spectra of AlN films of different thicknesses (50, 80 and 120 nm) as a function of incidence photon wavelength in the range 200-800nm. All the films exhibit good optical transparency with better than 80% at 550 nm and are excellent for optoelectronic devices therefore the optical characterization of these films were performed. The films show a sharp decrease of transmittance in the ultraviolet region due to the fundamental absorption of the light. It can be observed that the transmission of AlN films decreases and absorption edge of the transmittance shifts towards longer wavelength side in the ultraviolet region as the film thickness increases. This characteristic may be due to the increase of surface roughness and average grain size with the increase of film thickness. Besides, the interference phenomenon appeared in transmittance spectra of the films with higher thickness indicate a smooth and homogeneous surface of deposited films [12].

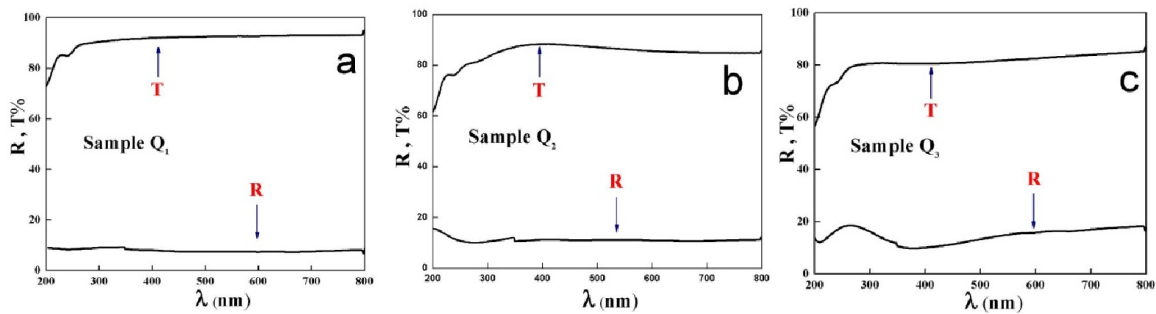


**Figure 5.** Transmittance (T) and reflectance (R) spectra of AlN thin films with different thicknesses deposited on quartz substrates: (a): 50 nm, (b): 80 nm and (c): 120 nm.

Now, we attempt to study the influence of film thickness on optical band gap energy of AlN films. For this purpose, in the first step, the normal incidence transmission and reflectance data of the

films were used for determination of optical absorption coefficient,  $\alpha$  values in the high absorption region by the following relation [30]:

$$\alpha = (1/d) \ln [(1-R)/T] \quad (2)$$

where  $d$ ,  $R$  and  $T$  are the film thickness, reflectance and transmittance respectively. Then, the graphs of absorption coefficient versus photon energy ( $h\nu$ ) are studied to evaluate the value of optical band gap energy ( $E_g$ ). In the high absorption region, absorption coefficient  $\alpha$ , is related to the energy  $h\nu$  of incidence photons by the relation [31, 32]:

$$\alpha h\nu = B(h\nu - E_g)^p \quad (3)$$

Where  $B$  is a parameter depending on the transition probability,  $p$  is an index that characterizes the optical absorption process and is theoretically equal to 1/2, 2, 3/2 or 3 for direct allowed, indirect allowed, direct forbidden and indirect forbidden transitions respectively. The usual method of determining band gap is to plot of a graph between  $((\alpha h\nu)^{1/p}$  and  $h\nu$ ) in accordance to equation (3) and look for that value of  $p$  which gives best linear graph in the band edge region. For the samples of this study, the best fit was obtained for  $p=1/2$  indicating a direct allowed transition. The band gap energies ( $E_g$ ) of AlN films were obtained by extrapolating the linear portion of the plots of  $((\alpha h\nu)^2$  versus  $h\nu$  to  $\alpha=0$ ). Figure 6 shows the variation  $((\alpha h\nu)^2$  with  $h\nu$ ) of the AlN films deposited on quartz substrates. It was observed that the corresponding  $E_g$  decreased from 5.54 eV to 5.35 eV with the increase of the film thickness. These values are smaller than the values of 6.2 and 5.7 reported [3, 10], for bulk and AlN with hexagonal structures respectively. This could be attributed to the introduction of defect states during the growth process [10]. Furthermore, these values are in good agreement with the band gap values as reported by many earlier workers on AlN thin films [10-12]. The decrease in the band gap in the present case may be due to the increase in particle size. The results obtained in this study are consistent with those reported in literature [1, 7-12] and indicate formation of transparent AlN thin films with wide optical band gap and low surface roughness which may be useful for applications in microelectronic devices.

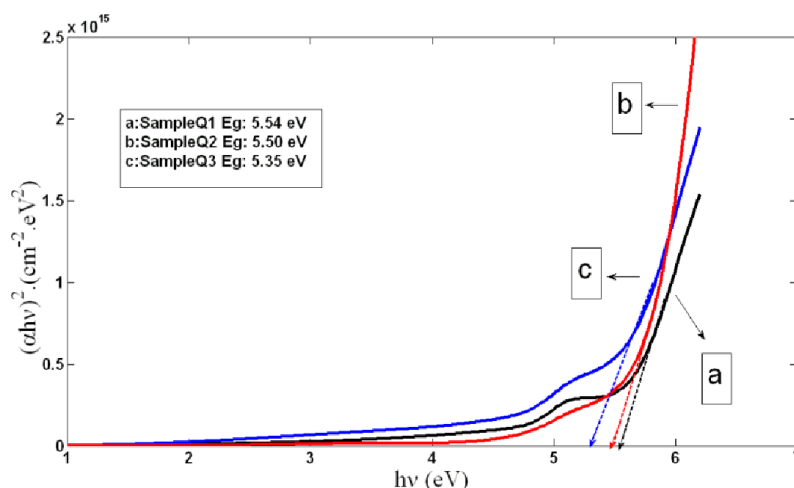


**Figure 6.** plot of  $(\alpha hv)^2$  versus photon energy ( $h\nu$ ) for AlN films with different thicknesses: (a): 50 nm, (b): 80 nm and (d): 120 nm.

## Conclusion

In summary, amorphous AlN thin films with different thicknesses in the range of 50-120 nm were grown onto quartz and silicon substrates by using single ion beam sputtering method. The influence of film thickness on the structural, morphological and optical properties of AlN films was studied. The XRD patterns confirm the amorphous nature of the AlN thin films. FTIR transmittance spectra confirmed the results obtained from the XRD. It is observed that the surface morphology of the films varies with the film thickness. The analysis of optical properties revealed the decrease of transmittance and optical band gap energy by enhancing of AlN film thickness may be due to the increase of particle size. The obtained results indicate formation of transparent AlN thin films with wide optical band gap and low surface roughness which may be useful for applications in microelectronic devices.

## References

- [1] D. L. Ma, H. Y. Liu, Q. Y. Deng, W. M. Yang, K. Silins, N. Huang, Y.X. Leng, *Vacuum*, 160,410(2019).
- [2] M. Durandurdu, *J. Am. Ceram. Soc.*,99,1594(2016).
- [3] H. Altuntas, T. Bayra, S. Kizir, A. Haider, N. Biyikli, *Semicond. Sci. Technol.*,31,075003 (2016).
- [4] M. Alevli, C. Ozgit, I. Donmez, N. Biyikli, *Phys. Status Solidi A.*,209,266(2012).
- [5] A. N. Redkin, E. E. Yakimov, D. I. Roshchapkin, V. Z. Korepanov, *Thin Solid Films.*,684, 15 (2019).
- [6] D. Cao, X. Cheng, Y. H. Xie, L. Zheng, Z. Wang, X. Yu, J. Wang, D. Shen, Y. Yu, *RSC Adv.*,5,37881 (2015).



- [7] A. Panddey, J. Kaushik, S. Dutta, A. K. Kapoor, D. Kaur, N. Huang, Y. X. Leng, *Thin Solid Films*, 666, 143 (2018).
- [8] K. A. Aissa, A. Achour, O. Elmazria, Q. Simon, M. Elhosni, P. Boulet, S. Robert, M. A. Djouadi, *J. Phys. D: Appl. Phys.*, 48, 145307 (2015).
- [9] R. J. Jimenez Rioboo, V. Brien, P. Pigeat, *J. Mater. Sci.*, 45, 363 (2010).
- [10] A. V. Singh, S. Chandra, A. K. Srivastava, B. R. Chakroborty, G. Sehgal, M.K. Dalai, G. Bose, *Appl. Surf. Sci.*, 257, 9568 (2011).
- [11] L. Duta, G.E. Stan, H. Stroescu, M. Gartner, M. Anastasescu, Z. Fogarassy, N. Mihailescu, A. Szekeres, S. Bakalova, I.N. Mihailescu, *Appl. Surf. Sci.*, 374, 143 (2016).
- [12] F. Hajakbari, M. M. Larijani, M. Ghoranneviss, M. Aslaninejad and A. Hojabri, *Jpn. J. Appl. Phys.*, 49, 095802 (2010).
- [13] Y. Gao, M. Hu, X. Chu, Q. Yan, *J. Mater. Sci. Mater. Electron.*, 24, 4008 (2013).
- [14] J. Sun, Q. Zheng, S. Cheng, H. Zhou, Y. Lai, J. Yu, *J. Mater. Sci. Mater. Electron.*, 27, 3245 (2016).
- [15] F. Hajakbari, M. T. Afzali, A. Hojabri, *Acta. Phys. Pol. A.*, 131, 417 (2017).
- [16] G. Sanal Kumar, N. Illyaskutty, S. Suresh, R. Sreeja Sreedharan, V.U. Nayar, V.P. Mahadevan Pillai, *J. Alloys Compd.*, 698, 215 (2017).
- [17] F. Hajakbari, A. Hojabri, *J. App. Chem. Res.*, 12, 58 (2018).
- [18] F. Hajakbari, M. Ensandoust, *Acta. Phys. Pol. A.*, 129, 680 (2016).
- [19] A. Hojabri, F. Hajakbari, Y. Ghodrat, *J. App. Chem. Res.*, 9, 103 (2015).
- [20] A. Hojabri, Z. Kavyani, M. Ghoranneviss, *J. Inorg. Organomet. Polym.*, 27, 53 (2017).
- [21] S. Jalili, F. Hajakbari, A. Hojabri, *J. Theor. Appl. Phys.*, 12, 15 (2018).
- [22] A. Hojabri, N. Haghghian, K. Yasserian, M. Ghoranneviss, *IOP Conf. Seri: Mater. Sci. Eng.*, 12, 012004 (2010).
- [23] S. Rashvand, A. Hojabri, *J. Inorg. Organomet. Polym.*, 27, 503 (2017).
- [24] A. Hojabri, M. adavi, F. Hajakbari, *Acta. Phys. Pol. A.*, 131, 386 (2017).
- [25] I. Horcas, J. M. Fernandez, J. G. Roderiguez, J. Colchero, J. G. Herrero, A. M. Baro, *Rev. Sci. Instrum.*, 78, 013705 (2007).
- [26] Y. Fu, X. Li, Y. Wang, H. He, X. Shen, *Appl. Phys. A.*, 106, 937 (2012).
- [27] M. Ben Amor, A. Boukhachem, A. Labidi, K. Boubaker, M. Amlouk, *J. Alloy. Compd.*, 693, 490 (2017).
- [28] Y. C. Teh, A. A. Saif, *J. Alloys Compd.*, 703, 407 (2017).
- [29] C. H. Chua, H. W. Wu, J. L. Huang, *Ceram. Intl.*, 42, 5754 (2016).

- [30]M. Karyaoui, A.Mhamdi, H.Kaouach, A.Labidi, A.Boukhachem, K. Boubaker,M.Amlouk, R.Chtourou, *Mater. Sci. Semicond. Process.*,30, 255(2015).
- [31]J. Tauc and A. Menth, *J. Non-Cryst. Solids.*,8, 569 (1972).
- [32]F. Hajakbari, F. Shafienejad, *Jpn. J. Appl. Phys.*, 55,035503(2016).